

# On the use of the balance equation for the computation of geopotential in the tropics

Y. RAMANATHAN, D. R. SIKKA and C. M. DIXIT

*Institute of Tropical Meteorology, Poona*

(Received 20 February 1970)

**ABSTRACT.** The 'balance equation' is numerically solved to compute the geopotential field using the stream function derived from the observed winds. Synoptic and semi-quantitative comparisons are made between the computed and the observed geopotential fields. The contribution of different terms (vorticity  $\beta$  and Jacobian) are evaluated separately. The case studied is one of SW monsoon situation and the patterns of the computed geopotential field at different levels are found to have good correspondence with the wind field as well as the observed geopotential field.

## 1. Introduction

Several workers (Philips 1958; Brown and Neilon 1961, Alaka *et al.* 1967; Baumhefner 1968) have derived the geopotential field from the wind field by solving the inverse balance equation. Miyakoda (1960) suggested that the determination of the geopotential by this method avoids fictitious disturbances which may occur in low latitude if the reverse procedure of obtaining the stream function from the geopotential is adopted. Thus, for the Indian region lying in the tropics, it would be worthwhile to compute the geopotential field from the stream field and compare the same with a manually analysed geopotential field. This diagnostic study was undertaken with this objective.

## 2. Method of computation

The balance equation using the non-divergent wind can be expressed in the following way —

$$\nabla^2 \phi = f \nabla^2 \psi - \beta U_\psi + 2 J \left( \frac{\partial \psi}{\partial x}, \frac{\partial \psi}{\partial y} \right) \quad (1)$$

where,  $\phi$  is the geopotential,

$\psi$  is a stream function,

$U_\psi$  is the zonal wind component derived from the stream function,

$\beta$  is Rossby parameter,

and  $J$  is the Jacobian operator.

For the solution of Eq. (1) boundary conditions have to be prescribed. Along the boundary we can either use the computed geopotential from the geostrophic approximation or manually analysed geopotentials.

In this study the latter procedure has been adopted.

The stream function required for the solution of Eq. (1) was obtained by solving the Poisson equation,

$$\nabla^2 \psi = \xi \quad (2)$$

The wind field was manually analysed in the form of stream lines and isotachs and the wind vector at grid points were picked up for the calculation of relative vorticity ( $\xi$ ). The area of the study was from 2.5°N to 27.5°N and 50°E to 110°E and the grid interval is 2.5° both along latitudes and longitudes. The northern boundary was kept south of the Himalayas.

The boundary conditions used for solving Eq. (2) is after version II of Hawkins and Rosenthal (1965). The accelerated Liebmann relaxation procedure was used for the solution of Eq. (1) and (2) with 1.72 as the over-relaxation factor and 0.05 as the residue limit. The finite difference scheme for the Laplacian was a five point one, and the Jacobian was computed by the nine point scheme of Arakawa (1963).

## 3. Discussion

The synoptic situation chosen for the study was on 15 and 16 June 1966 in which the chief feature was a monsoon depression in the north Bay of Bengal. Stream line and isotach charts were prepared for the levels 850, 700, 500 and 300 mb for the 00 Z observations of these days. It may be mentioned that although the wind data was satisfactory to the north of the centre of the depression upto 700 mb at least, there was no data south of the centre. Surface ship reports, satellite

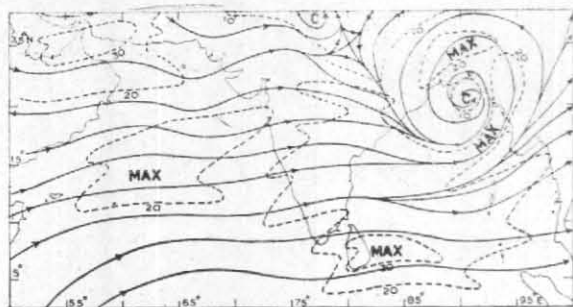


Fig. 1. Stream lines and isotachs for 850 mb on 16 June 1966 (00 Z)

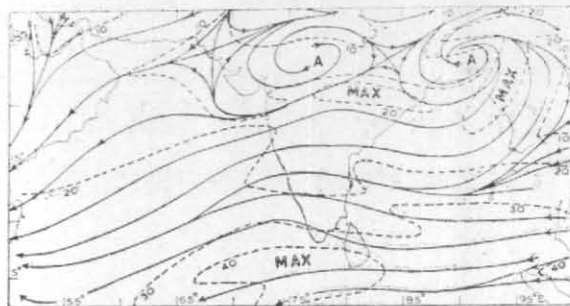


Fig. 4. Stream line and isotachs for 300 mb on 16 June 1966 (00 Z)

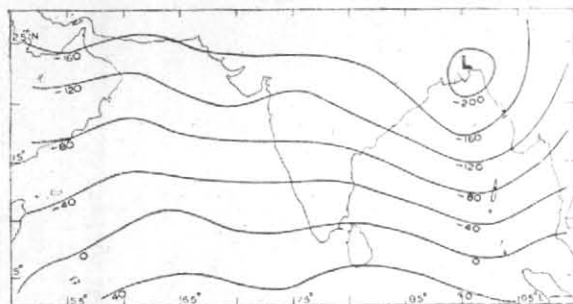


Fig. 2. Stream function for 850 mb ( $10^5$  m<sup>2</sup>/sec) on 16 June 1966 (00 Z)



Fig. 5. Stream function for 300 mb ( $10^6$  m<sup>2</sup>/sec) on 16 June 1966 (00 Z)

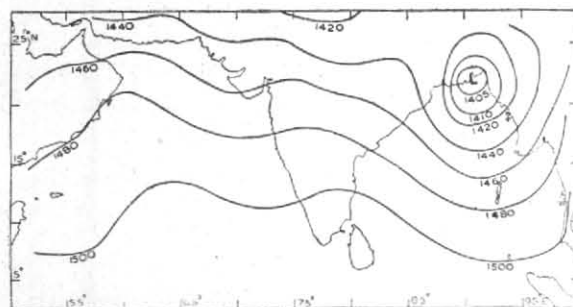


Fig. 3. Balanced geopotential (gpm) for 850 mb on 16 June 1966 (00 Z)

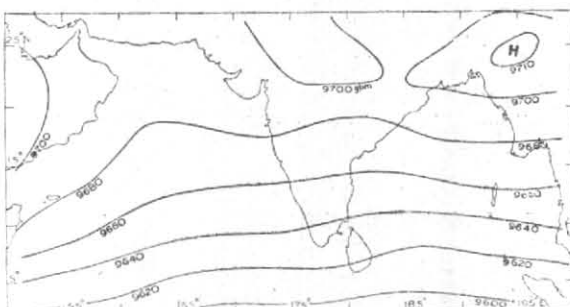


Fig. 6. Balanced geopotential (gpm) for 300 mb on 16 June 1966 (00 Z)

information and vertical continuity were used as additional tools in the analyses. Since the two dates yielded similar results the following discussion is confined to 16 June 1966. With a view to restricting the number of diagrams, details are discussed for 850 and 300 mb, which are representative of the lower and upper troposphere. The dominant feature of the synoptic situation on 16 June 1966 (00 Z) was a depression centred near  $20.5^{\circ}\text{N}$ ,  $90.5^{\circ}\text{E}$  extending to about 400 mb without much slope, apart from the monsoon trough in the lower troposphere and the subtropical ridge in the upper troposphere.

### 3.1. Comparison of computed geopotentials and stream functions

3.1.1. 850 mb chart—The stream line chart (Fig. 1) shows the depression located near  $20.5^{\circ}\text{N}$  and  $90.5^{\circ}\text{E}$ .

In association with it there is a north-south oriented trough in the Bay of Bengal along about  $90^{\circ}\text{E}$ . Other features of interest are—

(i) A trough in the Arabian Sea with axis between  $67.5$  and  $70^{\circ}\text{E}$ , (ii) A trough along  $77.5^{\circ}\text{E}$  near the northern boundary, (iii) Two ridges along

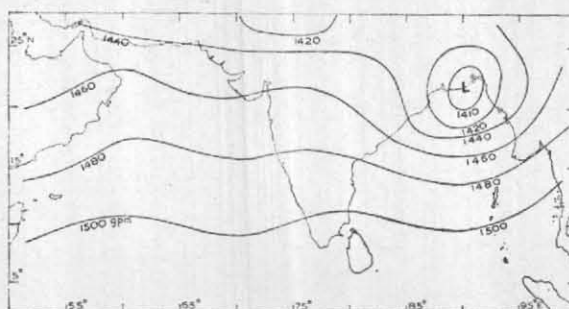


Fig. 7. Observed geopotential (gpm) for 850 mb on 16 June 1966 (00 Z)

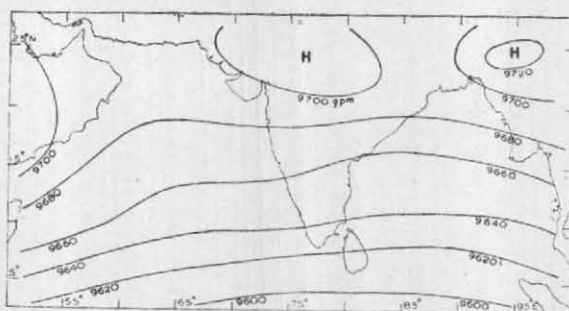


Fig. 8. Observed geopotential (gpm) for 300 mb on 16 June 1966 (00 Z)

about  $60^{\circ}\text{E}$  and  $75^{\circ}\text{E}$  and (iv) A strong wind belt between  $12^{\circ}$  and  $17^{\circ}\text{N}$  with a wind maximum over the Ceylon region. The stream function chart (Fig. 2) and the computed geopotential field chart (Fig. 3) generally depict the above features very well. The centre of the depression both in the stream function chart and the computed geopotential chart is somewhat north of its position in Fig. 1. The ridge in the Arabian Sea is somewhat more prominent in Fig. 3.

3.1.2. 300 mb chart—The chief features of the stream line chart (Fig. 4) are —

(i) Two anticyclonic circulations located near  $23^{\circ}\text{N}$ ,  $90^{\circ}\text{E}$  and  $24^{\circ}\text{N}$ ,  $77^{\circ}\text{E}$  and a weak trough in the easterlies located between them and (ii) A wind maximum in the easterlies, south of India. The stream function chart (Fig. 5) and the computed geopotential field (Fig. 6) show broad agreement with the stream line chart. The anticyclone over the Bengal region appears in both the charts though it is somewhat displaced eastward in the geopotential field. The other anticyclonic circulation appears only as a ridge in the stream function chart.

### 3.2. Comparison of the computed geopotential field with the actual geopotential field

The comparison of the computed geopotential field ( $\phi_B$ ) with the actual height field ( $\phi_A$ ) can be made either by comparing the two fields at the grid points or at the observing stations. Since the observed height field at a number of stations were not mutually consistent due to observational error, in this study a comparison of  $\phi_B$  and  $\phi_A$  fields was made only at grid points. For this purpose careful manual analyses of the observed geopotential field for 850, 700, 500 and 300-mb surfaces were made independently of the stream line charts. However, due to lack of height reports in comparison to wind reports and the mutual inconsistencies in the available height reports sufficient weightage to the wind data was given in the process of contour analysis. Generally, in manual analysis of the contours, the parallelism of the contours and the reported wind was kept in view though it was rather difficult to allow for the variation of the Coriolis parameter with latitude.

Figs. 7 and 8 show the hand analysed contour fields for 850 and 300 mb respectively.



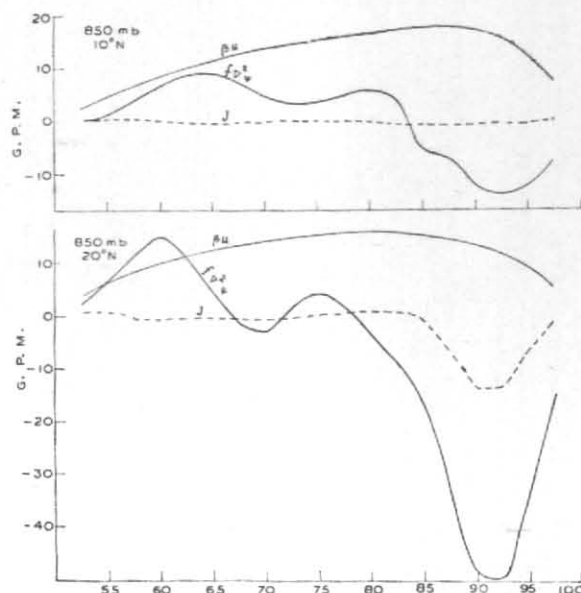


Fig. 9. Cross-sections along  $10^{\circ}$  N and  $20^{\circ}$  N showing effects of different terms in the forcing function for the solution of balanced geopotential at 850 mb on 16 June 1966 (OO Z)

TABLE 1

Root mean square difference between  $\phi_B$  and  $\phi_A$  and the highest differences

Level (mb)	Root mean square difference (gpm)	Highest difference (gpm)
850	6.2	16
700	4.7	15
500	10.2	34
300	6.7	20

A comparison of these with Figs. 3 and 6 shows several similarities and differences.

(1) The centre of the depression at 850 mb and the centres of the anticyclones at 300 mb are in agreement.

(2) The positions of the troughs and ridges at both the levels are in general agreement.

(3) The lowest grid point value in the field of the depression at 850 mb in  $\phi_B$  was 1398 gpm whereas in the  $\phi_A$  it was 1403 gpm.

(4) The highest grid point value in the anticyclone at 300 mb over Bengal in  $\phi_B$  was 9715 gpm and in  $\phi_A$  it was 9724 gpm. Thus it is found that in balanced height field derived from the wind, the low is slightly deeper and the high is slightly less intense than in the actual field.

The root mean square differences (R.M.S.D.) between the  $\phi_B$  and  $\phi_A$  fields and the highest differences at different levels are shown in Table 1.

TABLE 2

Root mean square difference values

Level (mb)	Root mean square difference between	
	$X\phi_A$ and $X\phi_B$ (gpm)	$Y\phi_A$ and $Y\phi_B$ (gpm)
850	6.1	5.3
700	4.9	5.1
500	9.2	8.6
300	4.7	5.7

In order to get an estimate about the agreement between the gradients of  $\phi_B$  and  $\phi_A$  at each grid point, central differences of  $\phi_B$  and  $\phi_A$  fields were computed. Let these be represented by  $X\phi_B$  and  $X\phi_A$  in east-west and  $Y\phi_B$  and  $Y\phi_A$  in north-south directions. The root mean square differences between  $X\phi_B$  and  $X\phi_A$  as well as between  $Y\phi_B$  and  $Y\phi_A$  are given in Table 2.

There was satisfactory agreement between the patterns of  $X\phi_B$  and  $X\phi_A$  as well as between the patterns of  $Y\phi_B$  and  $Y\phi_A$ . Tables 1 and 2 show that the R. M. S. D. values are highest at 500 mb. This is rather difficult to explain but may perhaps be due to weak gradient in the geopotential field at this level.

Since the contribution due to Jacobian term with the non-divergent wind was generally found to be small, it was decided to examine whether the inclusion of the total wind ( $u$  and  $v$ ) in the Jacobian term would make any appreciable

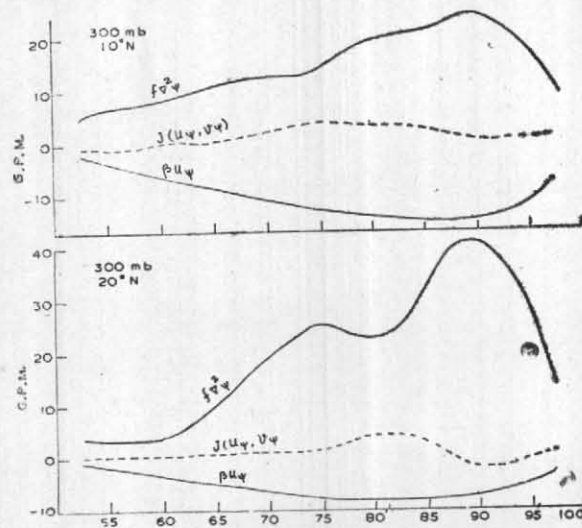


Fig. 10. Cross-sections along 10°N and 20°N showing effects of different terms in the forcing function for the solution of balanced geopotential at 300 mb on 16 June 1966 (00 Z)

change. However, this was not found to make any significant change in the computed geopotential field.

#### 4. Effect of different forcing terms

In order to study the effect of each term of the forcing function of Eq. (1), the solution of the equation was also obtained in four stages —

- (1)  $\nabla^2\phi_1 = 0$   $\phi_1$  on boundary equal to given boundary value of geopotential
- (2)  $\nabla^2\phi_2 = f\nabla^2\psi$ ,  $\phi_2 = 0$  on the boundary
- (3)  $\nabla^2\phi_3 = \beta\partial\psi/\partial y$ ,  $\phi_3 = 0$  on the boundary
- (4)  $\nabla^2\phi_4 = 2J\left(\frac{\partial\psi}{\partial x}, \frac{\partial\psi}{\partial y}\right)$   $\phi_4 = 0$  on the boundary

The solution  $\phi_1$  assesses the control of the solution by the prescribed boundary values;  $\phi_2$ ,  $\phi_3$ , and  $\phi_4$  isolate the effects of the three forcings in Eq. (1) separately. A comparison was made between  $\phi_2$  and  $\phi_3$  at each level. In general, the contribution due to the  $\beta$  term was opposite to that of  $f\nabla^2\psi$ .

The contribution due to the Jacobian term was negligible in general and attained significant values only near closed circulations and in the regions of confluence and diffuence. It was, generally of the same sign as that due to  $f\nabla^2\psi$ . For example, at 850 mb over the region of the depression the ratio of the contribution due to  $\nabla \cdot f\nabla\psi$  to that due to the Jacobian term was

M/P(N)LDGOB-6

on an average 2.5 and at 300 mb in the regions of the anticyclonic circulation this ratio was on an average 4.9.

Cross-sections along 10°N and 20°N giving the contribution of each term ( $\phi_2$ ,  $\phi_3$  and  $\phi_4$ ) are shown in Figs. 9 and 10 respectively for 850 mb and 300 mb. The small values of  $\phi_4$  at 10°N was due to the flow being nearly zonal in the case under study. This feature may not be expected in such cases where closed circulations are present. Near the equator only  $\phi_3$  from the  $\beta$  term can be of significance.

#### 5. Conclusion

The study shows that synoptically usable geopotential field can be derived from the wind field even in the case of the summer monsoon flow over the Indian area by solving the non-divergent balance equation despite possible errors in the computation arising from subjective wind analysis and boundary conditions.

A study of the effects of the various terms in the forcing function shows that generally the contribution from the Jacobian term is insignificant except near circulation centres and regions of confluence and diffuence. This suggests that in case of nearly zonal flow the linear balance equation,

$$\nabla^2\phi = \nabla \cdot (f\nabla\psi)$$

may give the same result as the complete non-divergent form of the balance equation even in tropical latitudes.

## REFERENCES

- |   |      |  |
|---|------|--|
| Alaka, M. A., Rubsam, D. T. and Fisher, G. E. | 1967 | <i>U.S. Weath. Bur. Mem.</i> WBTMTDL-8, pp. 20.  |
| Arakawa, A.                                   | 1963 | Computational design for long term numerical integration of the equations of fluid motion U.C.L.A. Dep. of met. contrib., 122. |
| Brown, John A. and Neilon, James R.           | 1961 | <i>Mon. Weath. Rev.</i> , <b>89</b> , pp. 83-90.   |
| Baumhefner, D. P.                             | 1968 | <i>Ibid.</i> , <b>96</b> , pp. 218-228.  |
| Hawkins, H. F. and Rosenthal, S. L.           | 1965 | <i>Ibid.</i> , <b>93</b> , pp. 245-252.  |
| Miyakoda, K.                                  | 1960 | Numerical solution of the Balance Equation. <i>Tech. Rep. Japan met. Agency</i> , 3.   |
| Phillips, N. A.                               | 1958 | <i>Geophysica</i> , <b>6</b> , pp. 479-501.  |
-